Synaptotagmin-like protein 2 gene promotes the metastatic potential in ovarian cancer

HYE YOUN SUNG[1], JIHYE HAN[1], WOONG JU[2*] and JUNG-HYUCK AHN[1*]

Departments of [1]Biochemistry and [2]Obstetrics and Gynecology, School of Medicine, Ewha Womans University, Yangcheon-gu, Seoul 158-710, Republic of Korea

Received January 12, 2016; Accepted March 28, 2016

DOI: 10.3892/or.2016.4835

Abstract. Ovarian cancer (OC) metastasis has unique biological behavior and most commonly occurs via the transcoelomic route. Previously, we established a mouse xenograft model of human ovarian carcinoma and analyzed alterations in gene expression during metastasis. Among the genes that were differentially expressed more than 2-fold in the xenografts compared with the SK-OV-3 cells, we selected *synaptotagmin-like protein 2 (SYTL2)* and investigated the mechanisms regulating its expression and its gene function in OC. The mRNA expression of *SYTL2* was significantly upregulated and the methylation of specific CpG sites within the *SYTL2* promoter was decreased in the metastatic implants from the ovarian carcinoma xenografts compared to wild-type SK-OV-3 cells. Treatment with the demethylating agent 5-aza-2'-deoxycytidine and/or the histone deacetylase inhibitor Trichostatin A induced upregulation of *SYTL2* in SK-OV-3 cells, implying that a DNA methylation-dependent epigenetic mechanism is involved in the regulation of *SYTL2* expression. We also found that overexpression of SYTL2 promoted metastatic potential, including increased migration and invasiveness in the ovarian carcinoma cells. Furthermore, we utilized publicly available gene expression data to confirm the correlation between *SYTL2* expression and poor prognosis in serous-type OC patients. Our findings provide novel evidence for the direct association of *SYTL2* with the metastatic potential of ovarian carcinoma cells and its influence on metastatic recurrence of OC.

Correspondence to: Professor Jung-Hyuck Ahn, Department of Biochemistry, School of Medicine, Ewha Womans University, 911-1 Mok-6-dong, Yangcheon-gu, Seoul 158-710, Republic of Korea
E-mail: ahnj@ewha.ac.kr

Professor Woong Ju, Department of Obstetrics and Gynecology, School of Medicine, Ewha Womans University, 911-1 Mok-6-dong, Yangcheon-gu, Seoul 158-710, Republic of Korea
E-mail: goodmorning@ewha.ac.kr

*Contributed equally

Abbreviations: OC, ovarian cancer; *SYTL2, synaptotagmin-like protein 2*; qRT-PCR, quantitative reverse-transcription polymerase chain reaction; BSP, bisulfite sequencing PCR; 5-aza-dC, 5-aza-2'-deoxycytidine; TSA, Trichostatin A; FBS, fetal bovine serum; DEGs, differentially expressed genes; DM, differentially methylated CpG site; HR, hazard ratio; SHD, Slp homology domain; GAP, GTPase-activating protein

Key words: synaptotagmin-like protein 2, DNA methylation, ovarian cancer, metastasis

Introduction

Ovarian cancer (OC) has the worst prognosis of all the gynecological cancers and it is the eighth leading cause of cancer-related death among Korean women (1,2). Despite the improvements in detection and the treatment of OC, an estimated 75% of women with the disease are first diagnosed with advanced-stage (III or IV) cancer, and the risk for recurrence after completion of primary therapy is 60% to 85%, resulting in a 5-year survival rate of <45% (3). Since no ovarian tissue remains after standard treatment, which includes total hysterectomy with bilateral salpingo-oophorectomy (4), all OC recurrences following primary treatment are from metastasis spread to other organs. Therefore, a better understanding of the molecular mechanisms that are involved in metastatic recurrence of OC will provide improvements in detection and treatment of OC.

Metastasis of OC most commonly occurs via the transcoelomic route, which is intraperitoneal seeding mediated by ascites (5,6). Although the mechanisms of metastatic recurrence are not well understood, the role of microenvironmental changes at the cancer implantation site is considered as one of the central mechanisms for intraperitoneal seeding of OC (7). Among several factors that change the tumor microenvironment, epigenetic alteration and consequent differential gene expression are being focused on as promising new targets in the treatment of advanced OC (8). Understanding pathophysiologic events at the epigenetic as well as the genetic level may elucidate the mechanisms of OC metastatic recurrence.

Previously, we established a mouse xenograft model to mimic human ovarian cancer metastasis by injecting SK-OV-3 human ovarian cancer cells into the peritoneal cavities of female nude mice and analyzed alterations in gene expressions during the metastasis of OC (9). We found that the expression patterns of certain genes in the xenografts reflect, to some

extent, the pathophysiological conditions of human metastatic OC (9). In the present study, we selected *synaptotagmin-like protein 2 (SYTL2)*, which was significantly upregulated in the xenografts during metastasis, for further investigation. Our results showed that the expression of *SYTL2* was regulated by epigenetic modification and aberrant overexpression of *SYTL2* induced metastatic potential in the ovarian carcinoma cells. Moreover, the clinical significance of *SYTL2* expression in OC patients with poor prognosis was confirmed by meta-analysis. Our findings provide novel insights into understanding the regulatory mechanisms and the role of *SYTL2* in OC and may offer a new therapeutic target and/or prognostic biomarker for the treatment of metastatic recurrence.

Materials and methods

Cell culture. The human ovarian cancer cell line SK-OV-3 was purchased from the American Type Culture Collection (ATCC; no. HTB-77; Manassas, VA, USA) and A2780 was purchased from the European Collection of Cell Cultures (cat no. 93112519; Wiltshire, UK).

SK-OV-3 cells were cultured in McCoy's 5A medium containing 10% fetal bovine serum (FBS), 100 U/ml penicillin, and 100 μg/ml streptomycin (all from Gibco-BRL, Rockville, MD, USA) in a 95% humidified air and 5% CO_2 atmosphere at 37˚C.

A2780 cells were cultured in RPMI-1640 medium (Welgene, Inc., Gyeongsangbuk-do, Korea) containing 10% FBS, 100 U/ml penicillin, and 100 μg/ml streptomycin (all from Gibco-BRL) in a 95% humidified air and 5% CO_2 atmosphere at 37˚C.

Ovarian cancer mouse xenograft model. All procedures for handling and euthanizing the animals used in this study were performed in strict compliance with the guidelines of the Korean Animal Protection Law and were approved by the Institutional Animal Care and Use Committee (IACUC) of Ewha Womans University School of Medicine. SK-OV-3 cells ($2x10^6$) suspended in culture media were intraperitoneally injected into 10 female nude mice (CAnN.Cg-*Foxn1*^{NU}, 4-6 weeks old). Four weeks after inoculation, the xenograft mice were sacrificed, and at least four implants adhering to the mesothelial surface of each mouse were harvested.

RNA preparation and quantitative reverse transcription-polymerase chain reaction (qRT-PCR). Total RNA was extracted from the metastatic implants of ovarian cancer mouse xenografts and SK-OV-3 cells using the RNeasy Mini kit (Qiagen, Inc., Valencia, CA, USA) according to the manufacturer's instructions. One microgram of total RNA was converted to cDNA using Superscript II reverse transcriptase and oligo-$(dT)_{12-18}$ primers (both from Invitrogen Life Technologies, Carlsbad, CA, USA) according to the manufacturer's instructions. qRT-PCR was performed in a 20 μl reaction mixture containing 1 μl cDNA, 10 μl SYBR *Premix EX Taq* and 0.4 μl ROX reference dye (50X; both from Takara Bio, Inc. Otsu, Japan), and 200 nM primers for each gene. The primer sequences were: *SYTL2* (forward), 5'-GGAGGTC TTCGTATTGGCTTTG-3'; *SYTL2* (reverse), 5'-CCATCTTC TCCCAGAGAGCAA-3'; GAPDH (forward), 5'-AATCCCAT CACCATCTTCCA-3'; and GAPDH (reverse), 5'-TGGACTCC ACGACGTACTCA-3'. The reactions were run on a 7500 Fast Real-Time PCR system (Applied Biosystems Life Technologies, Foster City, CA, USA) at 95˚C for 30 sec, followed by 40 cycles of 95˚C for 3 sec and 60˚C for 30 sec, and a single dissociation cycle of 95˚C for 15 sec, 60˚C for 60 sec, and 95˚C for 15 sec. All PCR reactions were performed in triplicate, and the specificity of the reaction was determined by melting curve analysis at the dissociation stage. Comparative quantification of each target gene was performed based on cycle threshold (CT) normalized to GAPDH using the $\Delta\Delta$CT method.

Messenger RNA microarray chip processing and analysis of gene expression data. Total RNA was extracted from the harvested metastatic implant of ovarian cancer mouse xenografts and SK-OV-3 cells using the RNeasy Mini kit and 1 μg of total RNA was amplified and labeled according to the Affymetrix GeneChip Whole Transcript Sense Target Labeling protocol. The resulting labeled cDNA was hybridized to Affymetrix Human Gene 1.0 ST arrays (Affymetrix, Santa Clara, CA, USA). The scanned raw expression values were background corrected, normalized, and summarized using the Robust Multiarray Averaging approach in the Bioconductor 'affy' package (Affymetrix). The resulting $\log_2$-transformed data were used for further analyses.

To identify differentially expressed genes (DEGs), we applied moderated t-statistics based on an empirical Bayesian approach (10). Significantly upregulated and downregulated DEGs were defined as genes with at least a two-fold difference in expression level between the xenograft cells and the wild-type SK-OV-3 cells after correction for multiple testing [Benjamini-Hochberg-false discovery rate (BH-FDR)-adjusted P-value <0.05] (11).

Finally, we excluded genes with a low expression level (maximum $\log_2$ expression level in a total of eight samples <7.0) from the list of DEGs.

Genomic DNA isolation and CpG methylation microarray. Genomic DNA was extracted from cell lines and tumor tissues using the QIAmp Mini kit (Qiagen), according to the manufacturer's instructions. For analysis of genome-wide screening of DNA methylation, the Illumina HumanMethylation450 BeadChip (Illumina, San Diego, CA, USA) was used to target 450,000 specific CpG sites. DNA methylation values were described as β-values, which were calculated by subtracting background using negative controls on the array and taking the ratio of the methylated signal intensity against the sum of both methylated and unmethylated signals. β-values ranged from 0 (completely unmethylated) to 1 (fully methylated) on a continuous scale for each CpG site. To identify differentially methylated CpG sites (DM), we applied the difference in mean β-value (Δβ; mean β-value in tumors - mean β-value in SK-OV-3). If the absolute difference of the mean β-values (|Δβ|) was >0.2, the site was defined as DM. We described a CpG site as hypermethylated if Δβ was >0.2, and hypomethylated if Δβ was <-0.2.

Bisulfite sequencing PCR (BSP). For bisulfite sequencing of the target promoter region of *SYTL2*, BSP was carried out using conventional PCR in a 50 μl reaction mixture containing

10 ng of bisulfite-modified genomic DNA, 1.5 mM $MgCl_2$, 200 μM dNTP, and 1 unit of Platinum *Taq* polymerase (Invitrogen Life Technologies), 1X Platinum *Taq* buffer and 200 nM of specific BSP forward and reverse primers for each gene. The BSP primers were designed using MethPrimer software (http://www.urogene.org/methprimer). For *SYTL2*, the BSP product is 345 bp (position in the human GRCh37/hg19 assembly: ch11, 85,437,289~85,437,633) and contained 4 CpG sites. The BSP primer sequences were: (forward), 5'-TTT TTGTTTTATGGGTATTTTTATTTGATA-3' and (reverse), 5'-AAAAAAACATTACTTTACCAACACTACAAC-3'. The reaction ran at 95˚C for 5 min, followed by 30 cycles at 95˚C for 30 sec, 60˚C for 30 sec and 72˚C for 30 sec, and a final elongation step at 72˚C for 5 min.

BSP products were purified using the QIAquick Gel Extraction kit (Qiagen) according to the manufacturer's instructions and ligated into the yT&A cloning vector (Yeastern Biotech, Taipei, Taiwan). The ligation products were used to transform competent DH5α *Esherichia coli* cells (RBC Bioscience Corp., Taipei, Taiwan) using standard procedures. Blue/white screening was used to select bacterial clones and BSP product-positive clones were confirmed by the colony PCR using BSP primers to verify insert size. Plasmid DNA was then extracted from at least six insert-positive clones using QIAprep Spin Miniprep kit (Qiagen) and sequenced using M13 primer to analyze methylation status at specific CpG site.

5-Aza-2'-deoxycytidine (5-aza-dC) and Trichostatin A (TSA) treatment. To demethylate methylated CpG sites, SK-OV-3 cells were treated with 0, 5, 10 and 20 μM of 5-aza-dC (Sigma-Aldrich, St. Louis, MO, USA) for 72 h. For co-treatment with 5-aza-dC and TSA, the cells were treated with 10 μM of 5-aza-dC for 72 h and then further treated with 0.5 μM of TSA for 24 h. The media were replaced daily.

Transient transfection. To establish a transient expression system, SK-OV-3 and A2780 cells were transfected with pAAV-CBA-*SYTL2* or pEGFP-N3 (Clontech, Mountain View, CA, USA) plasmid DNAs using Lipofectamine 2000 (Invitrogen Life Technologies). Briefly, the cells were plated at a density of 5-6x10^5 cells/well in 6-well plates and allowed to grow overnight. Two micrograms of each plasmid DNA and 5 μl of Lipofectamine 2000 were diluted separately in Opti-MEM medium (Gibco-BRL) to a total volume of 250 μl. The diluted plasmid DNAs and Lipofectamine 2000 were mixed and incubated at room temperature for 20 min to generate the transfection mixtures. The cells were washed with serum-free culture medium, and then the transfection mixtures were added to each well of the 6-well plates containing complete growth medium and incubated at 37˚C for 24 h in a 5% CO_2 incubator.

Transwell migration and in vitro invasion assays. After 24 h of transfection, the transfected cells were starved by serum deprivation. The cell migration assay was performed in 24-well Transwell plates containing inserts with a polycarbonate membrane with an 8.0 μm pore size (Corning Life Sciences, New York, NY, USA). After 24 h of serum deprivation, the cells were detached from the plates and resuspended in serum-free medium at a density of 2-4x10^6 cells/ml. One hundred microliters of the cell suspension was added to the upper compartment of the Transwell chamber. For each experiment, both chemotactic migration to medium containing 15% FBS and random migration in serum-free medium were assessed in parallel Transwell plates for 6 h at 37˚C in a 5% CO_2 incubator.

The *in vitro* invasion assay was performed using a BD BioCoat Matrigel invasion chamber (Becton-Dickinson, Franklin Lakes, NJ, USA). After 24 h of serum deprivation, the cells were detached from the plates and resuspended in serum-free medium at a density of 1-2x10^6 cells/ml. One hundred microliters of the cell suspension was added to the upper compartment of the invasion chamber, and 500 μl of culture medium containing 10% FBS was added to the lower compartment of the chamber. The migration through the Matrigel chamber was allowed to proceed at 37˚C for 24 h in a 5% CO_2 incubator.

After the incubation period, the cells that had not migrated from the upper side of the filter were carefully scraped away with cotton swabs. The cells on the lower side of the filter were fixed for 2 min using the Diff-Quick kit solution (Thermo Fisher Scientific, Inc., Waltham, MA, USA), stained with 1% crystal violet for 2 min, and washed twice with distilled water at room temperature. The images of the stained cells on the lower side of the membrane were acquired at x200 magnification in six different fields. For quantitative analysis, the stained cells were subsequently extracted with 10% acetic acid, and colorimetric measurement was performed at 590 nm.

Western blot analyses. Proteins (30-40 μg) were resolved using denaturing 8% sodium dodecyl sulfate-polyacrylamide gel electrophoresis (SDS-PAGE) and transferred to polyvinylidene fluoride (PVDF) membranes. The membranes were blocked in 5% skim milk in Tris-buffered saline with 0.1% Tween-20 and subsequently incubated overnight at 4˚C with the following primary antibodies: rabbit anti-*SYTL2* polyclonal antibody (1:1,000; Invitrogen), rabbit anti-β-actin monoclonal antibody (1:10,000; Sigma-Aldrich). After washing, the membranes were incubated with secondary antibodies conjugated to horseradish peroxidase for 1 h at room temperature. Chemiluminescence was detected using WestSave Star substrate (AbFrontier, Seoul, Korea) according to the manufacturer's instructions. Bands were visualized using the Luminescent Image Analyser LAS-300 (General Electric, Chicago, IL USA) and quantified using Image Gauge software (Fujifilm, Valhalla, NY, USA)

Meta-analysis. The association between the expression level of *SYTL2* and prognosis in serous-type ovarian cancer was validated using a recently developed meta-analysis package, curatedOvarianData (12), composed of 2,066 expression profiles and clinical data of ovarian cancer patients from 13 datasets including only serous ovarian cancer. Cox proportional hazards model was used to determine the hazard ratio for overall survival in each dataset and univariate meta-analysis was performed using a fixed effect model for combining hazard ratios.

Statistical analysis. All data are expressed as mean ± standard deviation of at least three independent experiments. Statistical analyses were carried out using GraphPad Prism5 soft-

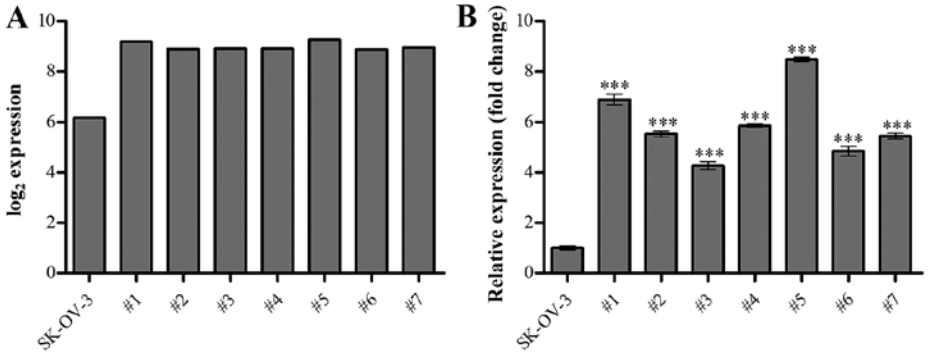

Figure 1. mRNA expression of *synaptotagmin-like protein 2 (SYTL2)* is upregulated in metastatic implants from xenograft mice. mRNA expression of *SYTL2* was measured by (A) expression microarray and (B) qRT-PCR. The error bars indicate the mean ± standard deviation (SD) of triplicate experiments. Statistical analyses were performed using one-way analysis of variance (ANOVA) and Tukey's multiple comparison post tests (***P<0.001). The metastatic implants from each mouse xenograft are labeled #1-#7 (n=7).

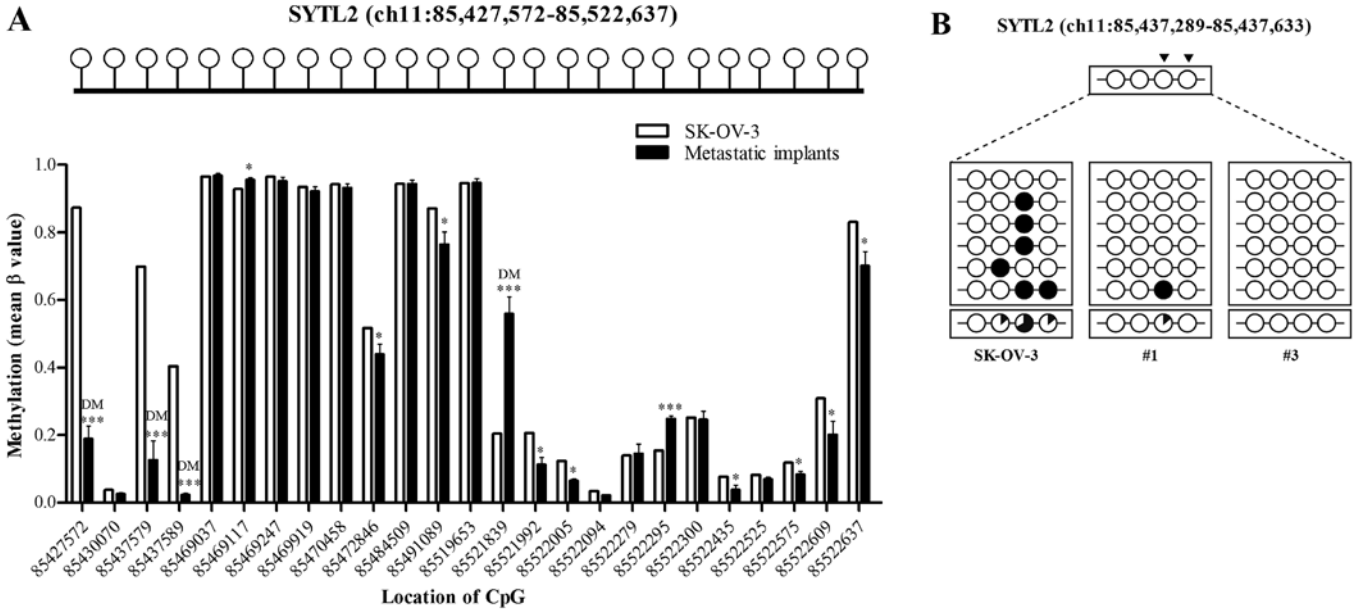

Figure 2. The status of DNA methylation within the *synaptotagmin-like protein 2 (SYTL2)* promoter is altered in metastatic implants. (A) The DNA methylation status of the *SYTL2* promoter region was analyzed using the Illumina HumanMethylation450 BeadChip that contains 25 specific CpG sites at positions 85,427,572-85,522,637 (the human GRCh37/hg19 assembly) within chromosome 11 (upper panel). Individual bars represent the mean β value of methylation at the corresponding CpG site within the *SYTL2* promoter (lower panel). Data are shown as the mean ± SD. Statistical analyses were performed using Bayesian t-tests (*P<0.05, ***P<0.001). (B) The DNA methylation status of the *SYTL2* promoter region located 85,437,289-85,437,633 within chromosome 11 was analyzed by BSP. Each circle represents a CpG dinucleotide. The methylation status of each CpG site is indicated with a black (methylated) or white (unmethylated) circle. The percentage of methylation at each site is indicated in a pie chart on the bottom line. The black segment of the pie chart indicates the percentage of methylated CpGs, whereas the white segment represents the percentage of unmethylated CpGs. Triangles above the circles in B indicate the same CpG sites that were used for the analysis using HumanMethylation450 BeadChip at positions 85,437,579 and 85,437,589. DM, differentially methylated CpG site.

ware (GraphPad, La Jolla, CA, USA) and the details of the statistical analysis for each data set is included in the figure legends. P-values <0.05 were considered to indicate statistically significant results.

Results

mRNA expression of SYTL2 is upregulated in metastatic implants from xenograft mice. Previously, we reported that mRNA expression was altered more than 2-fold in 937 genes, including 444 upregulated genes and 529 downregulated genes, in metastatic implants from ovarian carcinoma xenografts (9). Among the 444 upregulated genes, *SYTL2* mRNA expression was upregulated (6.6 to 8.6-fold) in the metastatic implants compared to wild-type SK-OV-3 cells (Fig. 1A). We confirmed overexpression of *SYTL2* by qRT-PCR, which showed significantly higher expression (4.3- to 8.5-fold) in all of the implants from the xenografts that we tested (Fig. 1B).

SYTL2 expression is regulated by epigenetic DNA methylation. Alteration of DNA methylation has been suggested to lead to aberrant changes in gene expression during cancer progression (13,14). Thus, we performed global DNA methylation profiling of the metastatic tumor implants and wild-type SK-OV-3 cells to determine if DNA methylation changes promoted high expression of the *SYTL2*

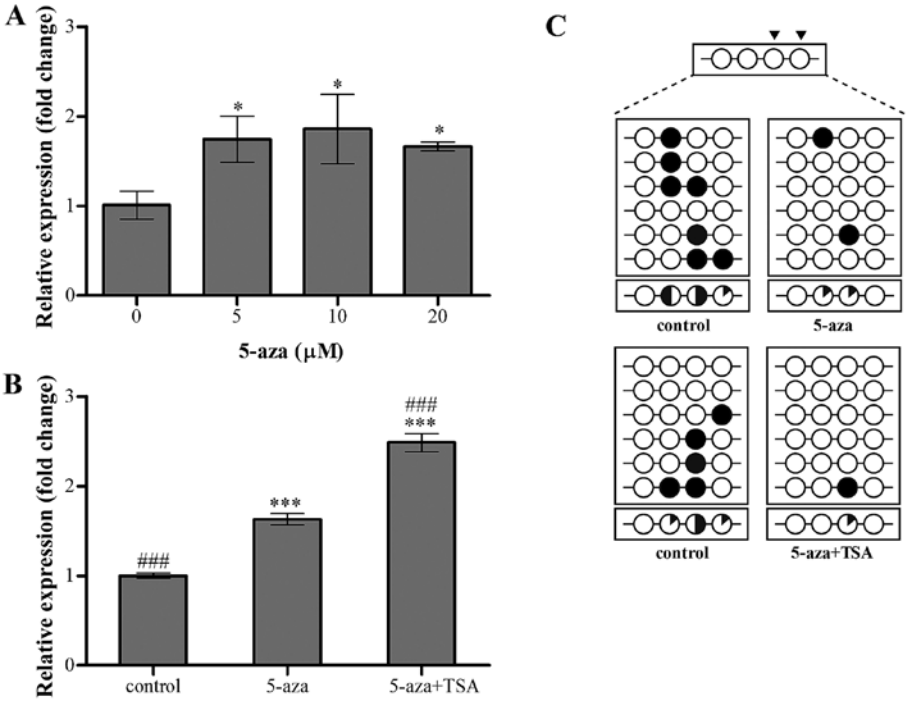

Figure 3. *Synaptotagmin-like protein 2 (SYTL2)* expression is increased following demethylation in SK-OV-3 cells. (A) The SK-OV-3 cells were treated for 72 h with various concentration of 5-aza-2'-deoxycytidine (5-aza), and the cells were treated with 10 μM of 5-aza for 72 h and (B) further treated with/without 0.5 μM of Trichostatin A (TSA) for 24 h. After treatment, mRNA expression of *SYTL2* was measured qRT-PCR. Data are shown as the mean ± SD (n=3). Statistical analyses were performed using one-way analysis of variance (ANOVA) and Tukey's multiple comparison post tests for comparing significance with the untreated control (*) or 5-aza treatment (#) (*P<0.05, ***P<0.001, $^{\#\#\#}$P<0.001). (C) After treatment of 5-aza and/or TSA, DNA methylation status of the *SYTL2* promoter region located at 85,437,289-85,437,633 was analyzed using bisulfite sequencing PCR (BSP). Each circle represents a CpG dinucleotide. The methylation status of each CpG site is illustrated by black (methylated) and white (unmethylated) circles. The total percentage of methylation at specific CpG sites is indicated as a pie chart. The black segment of the pie chart indicates methylated CpG percentage whereas the white segment represents the unmethylated CpG percentage.

gene during ovarian cancer metastasis. We used the Illumina HumanMethylation450 BeadChip, which covers 25 CpG sites within the promoter region of the *SYTL2* gene, which is located at 85,427,572-85,522,637 of chromosome 11 (the human GRCh37/hg19 assembly) (Fig. 2A). Among the 25 promoter CpG sites, 4 CpG sites were differentially methylated (1st, 3rd, 4th and 14th CpGs in Fig. 2A), and three out of the four CpGs were hypomethylated in ovarian metastatic implants compared to the wild-type SK-OV-3 cells (Fig. 2A). Next, we performed BSP of the *SYTL2* promoter region on chromosome 11 from 85,437,289-85,437,633 that contained 4 CpG sites in 2 representative tumor tissues (#1 and #3) and in the wild-type SK-OV-3 cell line. The results of BSP showed that the first CpG site was totally unmethylated in all tested samples, whereas the other three CpGs were hypomethylated in the metastatic tumor implants compared to wild-type SK-OV-3 cells (Fig. 2B). Consistent with the Beadchip analysis, DNA methylation of the CpGs at positions 85,437,579 and 85,437,589 was decreased in the metastatic implants compared to SK-OV-3 cells (Fig. 2B).

To determine whether altered mRNA expression of *SYTL2* is regulated by epigenetic modification, we treated SK-OV-3 cells with the DNA methyltransferase inhibitor 5-aza-dC and/or the histone deacetylase inhibitor TSA and quantified mRNA expression of *SYTL2* by qRT-PCR. After treatment with 5-aza-dC, mRNA expression of *SYTL2* was significantly increased (Fig. 3A). A synergic effect on *SYTL2* expression was also found after treatment with 5-aza-dC followed by TSA (Fig. 3B). After treatment with 10 μM 5-aza-dC and/or 0.5 μM TSA, decreased methylation status of the *SYTL2* promoter was confirmed using BSP (Fig. 3C). These results indicate that *SYTL2* gene expression was regulated by a DNA methylation-dependent mechanism.

Overexpression of SYTL2 induces aggressive phenotypes in human ovarian cancer cells. The SK-OV-3 and A2780 cells were transfected with pAAV-CBA-*SYTL2* and pEGFP-N3. The protein level of *SYTL2* expression was measured using western blot analysis. The cells transfected by pAAV-CBA-*SYTL2* expressed *SYTL2* at a much higher level than the cells transfected by pEGFP-N3; ~6.7-fold in SK-OV-3 cells and 4.8-fold in A2780 cells. The data confirmed that *SYTL2* was successfully transfected into both human ovarian cancer cell lines (Fig. 4A). To explore the function of *SYTL2* on metastasis, we performed *in vitro* migration and invasion assays using Transwell chambers. We observed a significant increase in migratory ability and invasion activity by overexpression of *SYTL2* in both human ovarian cancer cell lines, SK-OV-3 and A2780 cells (Fig. 4B and C). These data suggest that overexpression of *SYTL2* conferred migratory and invasive potential to the tumor cells.

High expression of SYTL2 is associated with poor prognosis of ovarian cancer patients. To examine the association between the expression level of *SYTL2* and overall survival in serous-type ovarian cancer patients, we performed

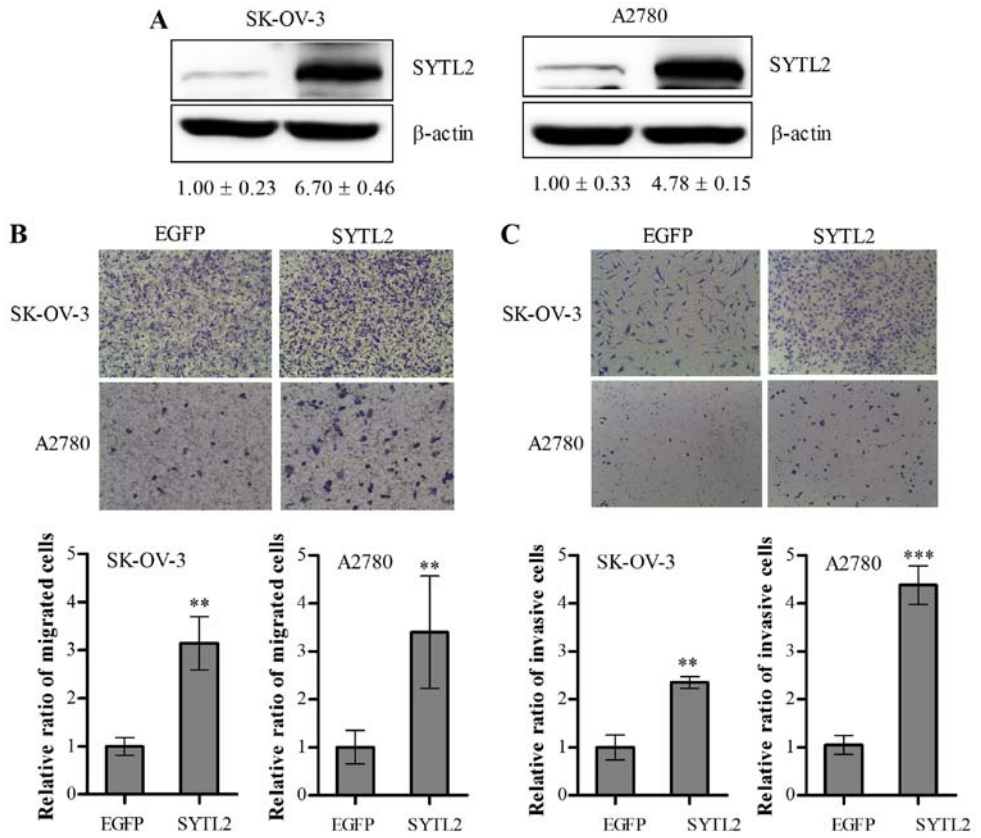

Figure 4. Overexpression of synaptotagmin-like protein 2 (SYTL2) promotes migration and invasiveness of ovarian cancer cells. (A) SYTL2 protein expression in the SK-OV-3 and A2780 cells transfected with pAAV-CBA-SYTL2 and pEGFP-N3 was determined by western blot analyses. The relative intensities of SYTL2 were quantified with Image Gauge software and normalized to β-actin. (B) Migration of serum-starved cells towards 15% serum-containing medium was determined by the Transwell assay. Cells that migrated through an 8-μm pore filter were fixed and stained with crystal violet. Representative images of migrated cells transfected with pAAV-CBA-SYTL2 and pEGFP-N3 are shown. Quantitative analysis of migrated cells was carried out by measuring the absorbance of the extracts of cell stained at 595 nm. (C) Invasion by serum-starved cells towards 10% serum-containing medium was determined using a Matrigel-coated invasion chamber. Data are shown as the mean ± SD of triplicate measurements. Statistical analysis was performed using a t-test (**P<0.01, ***P<0.001).

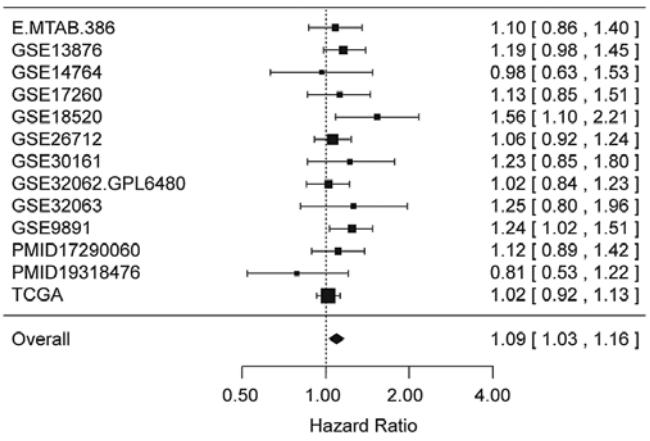

Figure 5. High expression of *synaptotagmin-like protein 2* (*SYTL2*) is associated with an increased risk of death in ovarian cancer patients. Forest plot of the significant association between increased risk of death and high expression of *SYTL2* in 2,066 serous-type ovarian cancer patients from 13 independent studies found in curatedOvarianData (12).

meta-analysis using curatedOvarianData (12), which includes >2,000 expression profiles and clinical data of ovarian cancer patients.

Meta-analysis confirmed that high expression of *SYTL2* was significantly associated with poor prognosis in serous-type ovarian cancer patients (Fig. 5). We found that the pooled hazard ratio (HR) estimate was significantly >1 for overall survival, indicating that the risk of death was incerased with increases in *SYTL2* expression. More specifically, the combined HR per 1 increment of gene expression was 1.09 (P=0.0048) and the expression change ranged from 3.8 to 14.7 (mean value, 5.8) in 13 datasets. Namely, the pooled HR was estimated at 1.65 by the expression change in the mean value of 5.8.

Discussion

SYTL2 was originally characterized as an effector protein for the Ras-related small GTPase Rab27 (15,16). It possesses an N-terminal Slp homology domain (SHD), Rab-binding region, and C-terminal tandem C2 domains, C2A and C2B (17,18). SYTL2 has been reported to be involved in transportation of melanosomes and secretory vesicles to the plasma membrane through the Rab27 binding activity of the SHD and the phospholipid binding activity of the C2A domain (19-21). Similarly, involvement of SYTL2 in polarized membrane trafficking has also been demonstrated in renal epithelial cells. *SYTL2*

regulates cell signaling and tubulogenesis through promoting trafficking of the signaling molecule podocalyxin to the apical surface in a Rab27-dependent manner (22). Recently, a Rab27-independent function of SYTL2 has been identified in renal epithelial cells. SYTL2 recruits Rapl GTPase-activating protein (GAP) to the plasma membrane through the C2B domain and controls cell size through modulating Rap-ezrin signaling (23).

In addition to the function of *SYTL2* in transportation to the plasma membrane, involvement of the *SYTL2* gene in cancer pathogenesis was recently reported. A systematic analysis of 61 Rab family and 223 Rab effector genes found that the Rab27 gene cluster was significantly deregulated in two main pathways (Ta pathway and carcinoma *in situ* pathway) during bladder cancer pathogenesis. In particular, *SYTL2* was downregulated in both pathways and was correlated with differentiation (24). Except for the study of bladder cancer, the involvement of *SYTL2* in other cancers has not been investigated, and the role of *SYTL2* in cancer remains largely unknown.

In the present study, *SYTL2* expression was significantly upregulated in the metastatic implants from ovarian carcinoma xenografts and the methylation status of specific CpG sites within the *SYTL2* promoter was highly decreased in the metastatic tissues compared to the wild-type SK-OV-3 cells. Treatment with the demethylating agent 5-aza-dC and/or the histone deacetylase inhibitor TSA induced upregulation of *SYTL2* in the SK-OV-3 cells by reduced DNA methylation within the *SYTL2* promoter, which indicates that a DNA methylation-dependent epigenetic mechanism is involved in the regulation of *SYTL2* expression. The results reported herein also revealed that overexpression of SYTL2 enhanced migratory and invasive potential in the ovarian carcinoma cells. Utilizing publicly available gene expression data, we confirmed the correlation between *SYTL2* expression and poor prognosis in serous-type ovarian cancer patients.

In conclusion, our findings provide novel evidence for *SYTL2* as an epigenetically regulated pro-metastatic factor that is associated with poorer patient survival. Although further investigations are required to understand the comprehensive molecular mechanisms of *SYTL2* in metastatic recurrence, this study suggests the potential use of *SYTL2* as a diagnostic and therapeutic target for metastatic recurrence of OC.

Acknowledgements

This study was supported by a grant of the Korean Health Technology R&D Project, Ministry of Health and Welfare, Republic of Korea (no. HI12C0050).

References

1. Jung KW, Won YJ, Kong HJ, Oh CM, Lee DH and Lee JS: Cancer statistics in Korea: incidence, mortality, survival, and prevalence in 2011. Cancer Res Treat 46: 109-123, 2014.
2. Yun JH, Lee HY, Park HW, Shin JW, Lee JM and Park CY: The analysis of prognostic factors in patients with epithelial ovarian cancer. Korean J. Obstet. Gynecol. 49: 566-571, 2006.
3. Siegel R, Naishadham D and Jemal A: Cancer statistics, 2012. CA Cancer J Clin 62: 10-29, 2012.
4. Tummala MK and McGuire WP: Recurrent ovarian cancer. Clin Adv Hematol Oncol 3: 723-736, 2005.
5. Feki A, Berardi P, Bellingan G, Major A, Krause KH, Petignat P, Zehra R, Pervaiz S and Irminger-Finger I: Dissemination of intraperitoneal ovarian cancer: discussion of mechanisms and demonstration of lymphatic spreading in ovarian cancer model. Crit Rev Oncol Hematol 72: 1-9, 2009.
6. Tan DS, Agarwal R and Kaye SB: Mechanisms of transcoelomic metastasis in ovarian cancer. Lancet Oncol 7: 925-934, 2006.
7. Jeon BH, Jang C, Han J, Kataru RP, Piao L, Jung K, Cha HJ, Schwendener RA, Jang KY, Kim KS, *et al*: Profound but dysfunctional lymphangiogenesis via vascular endothelial growth factor ligands from $CD11b^+$ macrophages in advanced ovarian cancer. Cancer Res 68: 1100-1109, 2008.
8. Balch C, Fang F, Matei DE, Huang TH-M and Nephew KP: Minireview: epigenetic changes in ovarian cancer. Endocrinology 150: 4003-4011, 2009.
9. Kim NH, Sung HY, Choi EN, Lyu D, Choi HJ, Ju W and Ahn JH: Aberrant DNA methylation in the IFITM1 promoter enhances the metastatic phenotype in an intraperitoneal xenograft model of human ovarian cancer. Oncol Rep 31: 2139-2146, 2014.
10. Smyth GK: Linear models and empirical bayes methods for assessing differential expression in microarray experiments. Stat Appl Genet Mol Biol 3: e3, 2004.
11. Benjamini Y and Hochberg Y: Controlling the false discovery rate: a practical and powerful approach to multiple testing. J R Stat Soc B 57: 289-300, 1995.
12. Ganzfried BF, Riester M, Haibe-Kains B, Risch T, Tyekucheva S, Jazic I, Wang XV, Ahmadifar M, Birrer MJ, Parmigiani G, *et al*: curatedOvarianData: clinically annotated data for the ovarian cancer transcriptome. Database (Oxford) 2013: bat013, 2013.
13. Jones PA and Baylin SB: The fundamental role of epigenetic events in cancer. Nat Rev Genet 3: 415-428, 2002.
14. Li L-C, Carroll PR and Dahiya R: Epigenetic changes in prostate cancer: implication for diagnosis and treatment. J Natl Cancer Inst 97: 103-115, 2005.
15. Fukuda M: Rab27 and its effectors in secretory granule exocytosis: a novel docking machinery composed of a Rab27·effector complex. Biochem Soc Trans 34: 691-695, 2006.
16. Kuroda TS, Fukuda M, Ariga H and Mikoshiba K: The Slp homology domain of synaptotagmin-like proteins 1-4 and Slac2 functions as a novel Rab27A binding domain. J Biol Chem 277: 9212-9218, 2002.
17. Fukuda M and Mikoshiba K: Synaptotagmin-like protein 1-3: a novel family of C-terminal-type tandem C2 proteins. Biochem Biophys Res Commun 281: 1226-1233, 2001.
18. Fukuda M, Saegusa C and Mikoshiba K: Novel splicing isoforms of synaptotagmin-like proteins 2 and 3: identification of the Slp homology domain. Biochem Biophys Res Commun 283: 513-519, 2001.
19. Torii S, Takeuchi T, Nagamatsu S and Izumi T: Rab27 effector granuphilin promotes the plasma membrane targeting of insulin granules via interaction with syntaxin 1a. J Biol Chem 279: 22532-22538, 2004.
20. Yu M, Kasai K, Nagashima K, Torii S, Yokota-Hashimoto H, Okamoto K, Takeuchi T, Gomi H and Izumi T: Exophilin4/Slp2-a targets glucagon granules to the plasma membrane through unique Ca^{2+}-inhibitory phospholipid-binding activity of the C2A domain. Mol Biol Cell 18: 688-696, 2007.
21. Kuroda TS and Fukuda M: Rab27A-binding protein Slp2-a is required for peripheral melanosome distribution and elongated cell shape in melanocytes. Nat Cell Biol 6: 1195-1203, 2004.
22. Yasuda T, Saegusa C, Kamakura S, Sumimoto H and Fukuda M: Rab27 effector Slp2-a transports the apical signaling molecule podocalyxin to the apical surface of MDCK II cells and regulates claudin-2 expression. Mol Biol Cell 23: 3229-3239, 2012.
23. Yasuda T and Fukuda M: Slp2-a controls renal epithelial cell size through regulation of Rap-ezrin signaling independently of Rab27. J Cell Sci 127: 557-570, 2014.
24. Ho JR, Chapeaublanc E, Kirkwood L, Nicolle R, Benhamou S, Lebret T, Allory Y, Southgate J, Radvanyi F and Goud B: Deregulation of Rab and Rab effector genes in bladder cancer. PLoS One 7: e39469, 2012.